Journal of Hydrology 669 (2026) 135111

Contents lists available at ScienceDirect

Journal of Hydrology

journal homepage: www.elsevier.com/locate/jhydrol

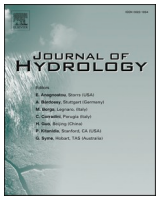

Research papers

Towards cooperation on transboundary rivers: achieving a win–win balance between upstream hydropower generation and downstream water demand under climate change

Tesfalem Abraham [a,f], Tunde Olarinoye [b], Andreas Hartmann [c], Harrie-Jan Hendricks Franssen [d], Yan Liu [d,e,*]

[a] Department of Water Resources and Irrigation Engineering, Institute of Technology, Hawassa University, 05, Hawassa, Ethiopia
[b] International Centre for Water Resources and Global Change (ICWRGC), 56068 Koblenz, Germany
[c] Institute of Groundwater Management, Technical University of Dresden 01069 Dresden, Germany
[d] Agrosphere (IBG 3), Forschungszentrum Jülich 52428 Jülich, Germany
[e] Soil Physics and Land Management Group, Wageningen University & Research, 6700 AA Wageningen, Netherlands
[f] Environmental and Atmospheric Sciences Research Group, Scientific Research Center, Al-Ayen University, Thi-Qar, Nasiriyah 64001, Iraq

ARTICLE INFO

This manuscript was handled by Ashok Mishra

Keywords:
Transboundary cooperation
Climate change
Water release scenarios
GERD
Omo-Gibe III
Tekeze

ABSTRACT

Transboundary river management is critical for international relations, sustainable energy development, and ecosystem management. Hydropower development, while meeting downstream water demand, is crucial for fostering cooperation among countries sharing water resources. However, addressing this challenge under the context of climate change poses significant complexities. This study investigates the cooperation regarding hydropower production and water releases under the potential impact of climate change. We project future streamflow by the calibrated HBV hydrological model in three transboundary rivers originating from Ethiopia: the Upper Blue Nile (UBN), Omo, and Tekeze rivers. Subsequently, we compute the hydropower potential (maximum hydropower energy within a specific period) by optimizing water release policies using the adapted 'Reservoir' R package. The hydropower potential and water release are analyzed based on 11 scenarios of water releases ranging from favoring the upstream country (Scenario 1) to benefiting downstream countries (Scenario 11) for the three example dams on the studied transboundary rivers: the Grand Ethiopian Renaissance Dam (GERD), Omo-Gibe III, and Tekeze dams. Our focus lies in identifying the cooperation ranges that provide optimal hydropower in the upstream and water release to the downstream among the varying water release policies within this scenario spectrum. The findings indicate that within an appropriate range for the minimum monthly water release threshold, the hydropower potential for the three study sites only has a small decrease, while the water release to downstream, especially for the driest month, can be 1.14–2.45 times larger compared to no water release constraints. For GERD and Omo-Gibe III, maintaining the monthly water release threshold of 30%-50% of the monthly flow is assumed to define the cooperation range in the historical periods. However, for Tekeze, the cooperation range is from 20% to 40% of the monthly water release. Due to climate change, the cooperation range for GERD and Omo-Gibe III is projected to decrease to 20–30% in future periods, whereas no significant impact is expected for Tekeze. The study reveals that future energy production of the hydropower dams on the transboundary rivers are influenced by the monthly minimum water release threshold, underscoring the need for adaptive cooperative strategies for both upstream and downstream countries in the face of climate change.

1. Introduction

Hydropower stands out as the most environmentally friendly energy source on a global scale. Registering over 10,400 hydropower dams across all continent (ICOLD, 2023), it contributes to nearly 70% of the world's total renewable energy supply (IEA, 2019). Globally there are

* Corresponding author.
E-mail address: yan.liu@fz-juelich.de (Y. Liu).

https://doi.org/10.1016/j.jhydrol.2026.135111
Received 29 April 2024; Received in revised form 5 February 2026; Accepted 8 February 2026
Available online 10 February 2026

around 286 rivers that cross the boundaries of two or more countries. In major river basins, over 70% of the dams either under construction or in the planning stages possess transboundary characteristics (Zarfl et al., 2015). Driven by such expansions it is crucial to plan the transboundary water resources governance, to enhance utilization and mitigate potential conflicts arising from shared water bodies. Accordingly, studies increased their focus to investigate the impacts of hydropower dams on transboundary rivers at various scales (Hennig, 2016; Llamosas and Sovacool, 2021). Water use priorities can significantly be affected particularly when sourced from transboundary rivers. Additionally, economic suitability of the transboundary rivers can influence the focus of water resource development for both upstream and downstream countries. A particular example is from the Mekong region showed a reliance of upstream nations for hydropower development, whereas the downstream side has heavily focused on irrigation development (Ly et al., 2022). Over the Nile basin, downstream countries like Egypt and Sudan have developed hydropower and irrigated agriculture sectors. In contrast, historically economically challenged upstream nations like Ethiopia, lag in water resource development. The Rhine in Europe, which traverses multiple countries stands as an example of successful and equitable transboundary river development (Chen et al., 2021). Upstream countries predominantly harness the river for hydropower, and the middle Rhine is massively used for domestic transportation, while the lower Rhine is heavily utilized for industrial water supply, and ports.

In recent decades, the global search for clean and sustainable energy has catalyzed the construction of numerous large hydropower dams, particularly on transboundary rivers (Zarfl et al., 2015). Iconic projects such as the Itaipu Dam on Parana River, the Grand Ethiopian Renaissance Dam (GERD) on Upper Blue Nile (UBN) river, and Nam Theun 2 Dam on Mekong River represent a paradigm shift in the energy sector. However, the proliferation of dams on transboundary rivers has introduced a complex interplay of cooperation and conflict among riparian nations, significantly shaping the geopolitical landscape (Giordano et al., 2014; Llamosas and Sovacool, 2021). Exemplifying successful collaboration, the Itaipu Dam stands as a joint endeavor by Brazil and Paraguay, not only yielding political advantages but also resolving a longstanding border conflict in the Paraná region (Gerlak et al., 2020; Ribeiro, 2017). Similarly, the Vuoksi River's cooperative management between Finland and Russia serves as a model, averting border conflicts and fostering basin-wide cooperation (Korjonen-Kuusipuro, 2011). Conversely, the construction of hydropower dams on transboundary rivers is not without challenges. For example, the Baglihar Dam project on a tributary of the transboundary Indus River in the early 2000s exemplifies the contentious nature of these ventures, heightening tensions between India and Pakistan without escalating into open warfare (Sinha, 2006). In arid Egypt, the High Aswan Dam, boasting an impressive 169 billion cubic meters (bcm) reservoir capacity, faces challenges as an annual evaporation loss of over 10 bcm raises concerns about ecosystem preservation (El-Magd and Ali, 2012). Ethiopia's GERD, the largest hydropower project in Africa, signifies the country's economic aspirations but triggers tensions with downstream. Therefore, such challenges call for a cooperative development and management of hydropower projects for maximizing their benefits and reducing risks of potential conflicts (Basheer et al., 2021; Ghoreishi et al., 2023; Wei et al., 2022).

Climate change has emerged as a major global concern, with far-reaching implications for various sectors, including water resources and energy production (IPCC, 2022). As hydropower remains a cornerstone of renewable energy strategies globally, understanding how climate-induced alterations in streamflow impacting its efficiency and reliability is crucial for sustainable energy development. Hydropower generation relies on consistent and predictable streamflow to optimize the performance of dams and turbines. The fluctuations in streamflow magnitudes, induced by climate change, have the potential to reduce water availability and consequently resulting in a decline in annual hydropower generation (Dallison et al., 2021). Additionally, extreme events such as floods and droughts, influenced by climate change, can pose operational challenges and affect the long-term sustainability of hydropower systems on the transboundary settings (Ly et al., 2022; Munia et al., 2020; Qin et al., 2020). Climate change further complicates energy generation and potential of hydropower, when particularly dealing with projects on transboundary rivers (Qin et al., 2020; Shu et al., 2018; Zhong et al., 2020). A study showed the global-scale stress induced by climate change on transboundary water resources, highlighting the interconnected challenges faced by regions sharing river basins (Munia et al., 2020). Considering inherent uncertainties in predictions of water resources and the corresponding energy potential, there is a need to integrate scenario-based hydropower operation for transboundary river management (Ly et al., 2022). In addition, the development of adaptive and mitigative strategies for climate change impact is crucial, especially concerning water resources and renewable energy. While existing studies have predominantly focused on adapting to climate change by increasing the proportion of hydropower generation to reduce greenhouse gas emissions (Shu et al., 2018), there remains a research gap in understanding strategies to optimize hydropower operation considering the need from both upstream and downstream countries of a transboundary river. Additionally, providing a feasible water release considering seasonal patterns to downstream and management of transboundary rivers in response to climate change is a crucial aspect. Managing hydropower in transboundary settings is contentious, requiring careful consideration of multiple interrelated factors. Future uncertainties related to climate change may severely impact hydropower operations on transboundary rivers, further complicating their management. Moreover, in cases where upstream and downstream countries lack cooperative agreements, these challenges can escalate into conflicts. Despite these complexities, no previous studies have clearly developed strategies to optimize hydropower production and water release scenarios in a way that balances upstream and downstream benefits under climate change.

With the intensified demand for water, reaching agreements on transboundary rivers allocations has become a challenge (Yuan et al., 2020). A study has reviewed the nature of conflicts along the major transboundary rivers such as the Nile river, Mekong river, and the Columbia River (Wei et al., 2022). One significant facet of this conflict lies in the need to strike a balance between upstream power generation and downstream water demands. Despite the completion of the reservoir filling, the GERD in Ethiopia is one example for the lack of agreement between the upstream (Ethiopia), and downstream countries (Sudan and Egypt) (Basheer et al., 2021). Several rounds of negotiations occurred between November 2019 to June 2020 initiated by the US government based on the Washington draft proposal, and later by the African Union, yet, the three countries have not reached an agreement. Key points of contention involve the correlation between the GERD agreement and prospective water development rights in Ethiopia, the interconnection between the GERD agreement and a lasting water allocation, and the duration of the agreement (Basheer et al., 2021). In addition, different case studies from the global contexts showed the complicated nature of conflicts on transboundary setting (Giordano et al., 2014; Llamosas and Sovacool, 2021). For example the experiences of regions such as the Mekong River basin (Soukhaphon et al., 2021), and Indus River (Sinha, 2006), exemplify the global significance of these challenges. In each case, factors such as legal frameworks, historical water use patterns, and socio-economic considerations, future development plans and climate change, contribute to the complexity of negotiations. Despite the successful examples of cooperation for energy production and water release between upstream and downstream countries in the historical periods, little is known about how climate change-induced alterations in energy production and water release could impact future cooperation. Additionally, to our knowledge, there has been no study addressing how projected climate change could alter water release from hydropower dams and its consequent impact on the cooperation for transboundary rivers.

In this study, we present an analysis of the impacts of climate change on scenario-based hydropower generation and water release on transboundary rivers. We examined various scenarios for potential dam operations on the transboundary rivers and assessed the influence of climate change on energy production and water demand for both upstream and downstream countries. We applied our framework to three example transboundary rivers originating from Ethiopia: the Upper Blue Nile, Omo, and Tekeze rivers. In this regard, we developed a new strategy by using the exploration of energy production under different water release scenarios to identify the optimal balance (cooperation range) between maximizing energy production and ensuring water security in the face of climate change. Determining this optimal balance holds the potential to enhance energy production in the upstream while simultaneously meeting the water demands of downstream countries. This, in turn, contributes to fostering cooperation and trust in the operation and management of transboundary hydropower projects amid changing climatic conditions.

2. Study sites

We test our framework (Sect. 3) that balances hydropower generation for the upstream and water release for the downstream with hydropower development of three major transboundary rivers: the Blue Nile, Tekeze, and Omo River (Fig. 1) originated from Ethiopia, a highland country situated in East Africa forming its large rivers with a transboundary nature (Fig. 1). The construction of the Grand Ethiopian Renaissance Dam (GERD) on the transboundary Blue Nile River positions it as the largest hydropower project in Africa, boasting a power capacity of 5,150 MW and a reservoir storage of 74 bcm (billion cubic meters) (Basheer et al., 2021). The Blue Nile contributes around 57% of the Nile streamflow as measured near the Sudanese-Egyptian border (NBI, 2012). The Omo River, the third-largest river in Ethiopia, flows from central Ethiopia to the southwest, ultimately reaching the border with Kenya (Fig. 1). The Omo-Gibe III hydropower dam, situated on the Omo River, boasts a power capacity of 1,870 MW and a reservoir storage of 14.7 bcm, establishing it as the second-largest hydropower facility in Ethiopia (Anebo et al., 2023). Tekeze, the fourth-largest river in Ethiopia, serves as a significant tributary of the Atbarah River, flowing towards Sudan (Fig. 1). The Tekeze-Atbarah basin contributes 13% of the total Nile River flow (Wheeler et al., 2020). The Tekeze Dam, located in North Ethiopia on the Tekeze River, has a power capacity of 300 MW and a reservoir storage of 9.3 bcm.

In Table 1, we summarized all the reservoir and dam-related variables obtained from openly accessible sources and studies (Ali et al., 2023; Annys et al., 2020; Antonio et al., 2018; Lazin et al., 2023; Peila et al., 2019). They include reservoir storage capacity, installed turbine capacity, and other relevant variables (Table 1) from the three hydropower dams, which are used as the parameters for the hydropower simulation model (Sect. 3.3) to calculate hydropower potential. The three dams, GERD, Omo-Gibe III and Tekeze are built on ground level or datum of 500 m, 660 m, and 971 m above sea level respectively. More description on the physical structure of three dams is shown in Fig. S1 of supplementary information.

3. Material and methods

The whole methodological framework includes three main parts (Fig. 2): i) the hydrological modeling part, which illustrates the hydrological model, forcing and model parameter confinement for streamflow simulations in the historical and future periods; ii) the hydropower potential modeling part, which shows the adapted hydropower potential model and illustrations of scenarios for hydropower generation optimization by introducing water release constraints (details are provided in Sect. 3.3); and iii) the hydropower – water release cooperation part, which discusses how the cooperation shifts from historical to future period due to climate change.

Table 1
Dam and reservoir characteristics of the three studied sites.

Variables	GERD	Omo-Gibe III	Tekeze
Reservoir storage capacity (Mm^3)	74,000	14,700	9,293
Live reservoir storage capacity (Mm^3)	59,200	11,750	5,300
Maximum surface area of reservoir (km^2)	1,874	210	155
Maximum hydraulic head (m)	80	210	162
Maximum reservoir depth (m)	140	250	185
Datum or Ground level (m.a.s.l)	500	660	971
Maximum water release through turbine (Mm^3/month)	11,563	2,462	570
Installed turbine capacity (MW)	5,150	1,870	300
Turbine efficiency (–)	0.95	0.95	0.95
Mean historical annual inflow (Mm^3/year)	65,724	13,026	3,583

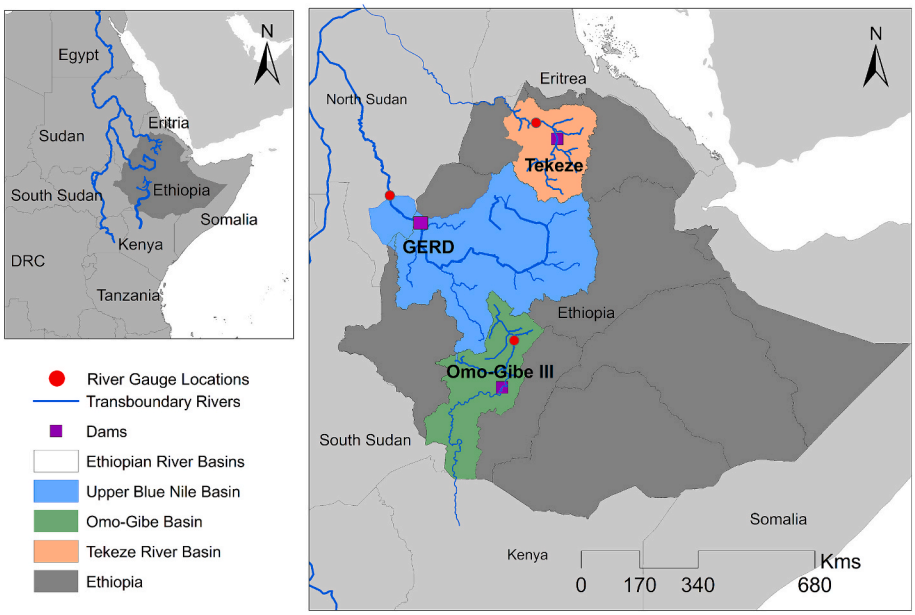

Fig. 1. Locations of the three investigated transboundary rivers and the associated hydropower dams.

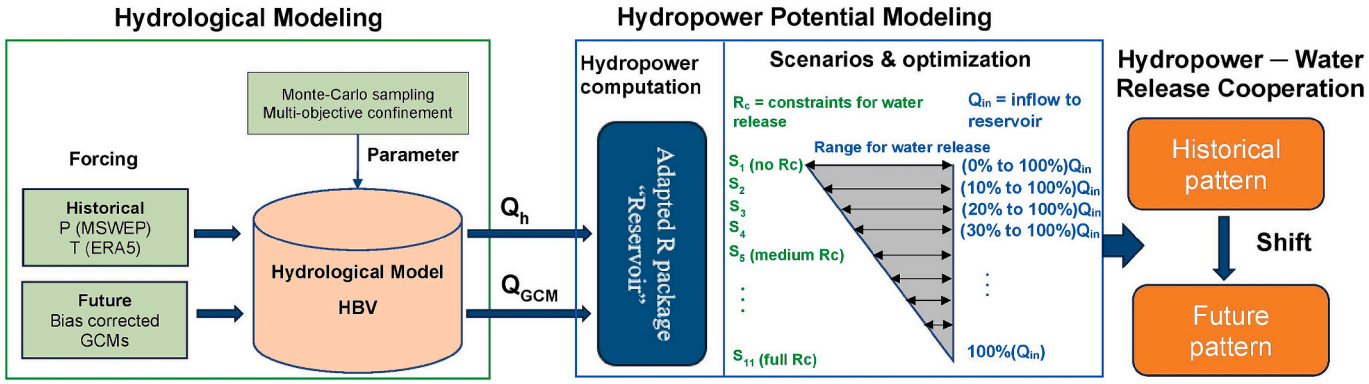

Fig. 2. Schematic diagram showing the methodological framework including hydrological modeling, hydropower potential modeling, and recommendations for hydropower-water release cooperation on the transboundary rivers in the historical and future periods.

3.1. Data

To derive the optimal parameters for the hydrological model, we calibrated the model using observed streamflow of the three transboundary rivers. We utilized inputs including precipitation, potential evapotranspiration, and daily streamflow for the calibration of the hydrological model (Table 2). Due to a lack of sufficient precipitation data in the three basins, we employed a global daily precipitation product from the Multi-Source Weighted-Ensemble Precipitation (MSWEP) version 2 at a 0.1° resolution (Beck et al., 2019). The MSWEP global precipitation product has been adequately utilized in recent studies to represent the rainfall climatology of Ethiopia (Aniley et al., 2023), and for transboundary basins (Abraham et al., 2025; Abraham and Liu, 2025; Basheer et al., 2023). For the calculation of potential evapotranspiration (PET), we applied the Hargreaves equation (Hargreaves and Samni, 1982), which relies solely on temperature data and radiation. We collected observed temperature data for the Omo and Tekeze basins from the National Meteorological Service Agency (NMSA) of Ethiopia. However, the Upper Blue Nile (UBN) basin lacks sufficient temperature data for PET calculations. For this reason, we relied on hourly temperature data from ERA5, which provides good spatial coverage, to estimate PET for the historical period. To further assess the reliability of ERA5 data, we evaluated it against observed temperature data from the Omo and Tekeze basins. The evaluation involved analyzing daily and monthly correlations (R^2) with observed temperatures, as well as comparing yearly mean values of observations and ERA5 temperature (Table S2). The strong performance of ERA5 in these basins supports its utility for the UBN basin, where observed temperature data are scarce. Streamflow observations for the Omo and Tekeze rivers were obtained from the Ministry of Water, Irrigation, and Electricity of Ethiopia (MoWIE). Due to restrictions on streamflow measurement data by the state for the UBN river, we utilized the best simulated streamflow at the Eldiem station from the study conducted by Ali et al. (2023).

Table 2
Inputs of historical data for the hydrological model calibration and PET calculation.

Inputs	Time	Spatial Resolution	Temporal Resolution	source
Precipitation (MSWEP V2)	1979–2020	0.1°	daily	www.gloh2o.org/mswep (last accessed on Jan 15, 2024)
Streamflow	1986–2014	point	daily	MoIWE and Ali et al. (2023)
Temperature (ERA5)	1940 to present	0.25°	hourly	cds.climate.copernicus.eu/ (last accessed on Jan 20, 2024)
Temperature (Obs)	1981–2005	Stations scale	daily	NMSA

3.1.1. Climate data selection

The forcing data, such as precipitation and temperature for the future periods, were utilized from the Global Climate Models (GCM). The GCMs were further downscaled into the Regional Climate Model (RCM) by the Coordinated Regional Climate Downscaling Experiment (CORDEX) project for Africa. We utilized a downscaled Regional Climate Model (RCM) dataset from the deriving models under CORDEX Africa project. The RCM datasets are accessible at a spatial resolution of 0.44° and temporal resolutions ranging from daily to monthly (Table 3). The RCM datasets for both precipitation and temperature are retrieved from the Earth System Grid Federation under the German Climate Computing Center (ESGF-DKRZ) at https://esgf-data.dkrz.de/search/cordex-dkrz/. The RCM data are the most reliable climate data and are frequently applied to investigate the impact of climate change on water resources in these regions (Adera and Alfredsen, 2020; Paulos et al., 2022; Teferi et al., 2015). Initially, we extracted 10 candidate RCM models that are commonly used in the regions for the three transboundary basins. Subsequently, we assessed the precipitation data of these 10 RCMs alongside the MSWEP precipitation for the historical periods (1981–2005) by comparing their annual averages and their correlation performances on the daily and monthly scale for the three basins (Table S1). Finally, we selected the top five RCMs (Table 3) that can well reproduce the seasonal variability based on maximum correlation (R^2

Table 3
Description of the selected RCM precipitation and temperature products from the CORDEX Africa for historical (1981–2005) and future (2025–2100) periods.

Model	Driving model	RCM Model	Time Period	Spatial Resolution	Source
RCA4_CNRM	CNRM-CERFACS-CNRM-CM5	RCA4	historical and future	0.44°	ECGF-DKRZ
RCA4_CSIRO	CSIRO-QCCCE-CSIRO-Mk3-6-0				
RCA4_GFDL	NOAA-GFDL-GFDL-ESM2M				
RCA4_MIROC5	MIROC-MIROC5				
RCA4_NorESM	NCC-NorESM1-M				

values) and long term annual average values.

3.1.2. Bias correction

After a careful selection of RCMs through comparisons with observations (MSWEP) in the historical period at daily, monthly and annual scale, the selected five RCMs still have certain biases. In this study, we use the scaled distribution mapping (SDM) (Switanek et al., 2017) to do bias corrections for precipitation and temperature. The main reason of using SDM is that, compared to quantile mapping (QM), e.g., quantile delta mapping (QDM), SDM makes no assumption regarding stationarity and it scales the observed distribution by raw model projected changes in magnitude, rain-day frequency (for precipitation), and likelihood of events (Switanek et al., 2017). Therefore, it can better preserve changes projected by RCMs (Carrillo et al., 2023; Casanueva et al., 2020; Gou et al., 2022; Switanek et al., 2017; Zhao et al., 2023). Casanueva et al. (2020) showed that SDM can preserve better the raw signals for the different indices and variables than other applied bias correction methods and Switanek et al. (2017) suggested SDM outperforms traditional QM and QDM.

We follow the standard procedure of SDM described in Switanek et al. (2017) to conduct bias corrections for the basin averaged daily precipitation and minimum and maximum daily temperature. Precipitation is scaled by a multiplicative amount, while temperature is scaled by an absolute amount. Gamma and normal distributions are used to fit the distributions of precipitation and temperature, respectively. Please refer to Switanek et al. (2017) for details and equations of SDM. SDM includes seven key steps to do the bias correction for precipitation and temperature as illustrated in Fig. 3 and the detailed equations (Eq. S1-S12) are provided in the supplementary information (SI).

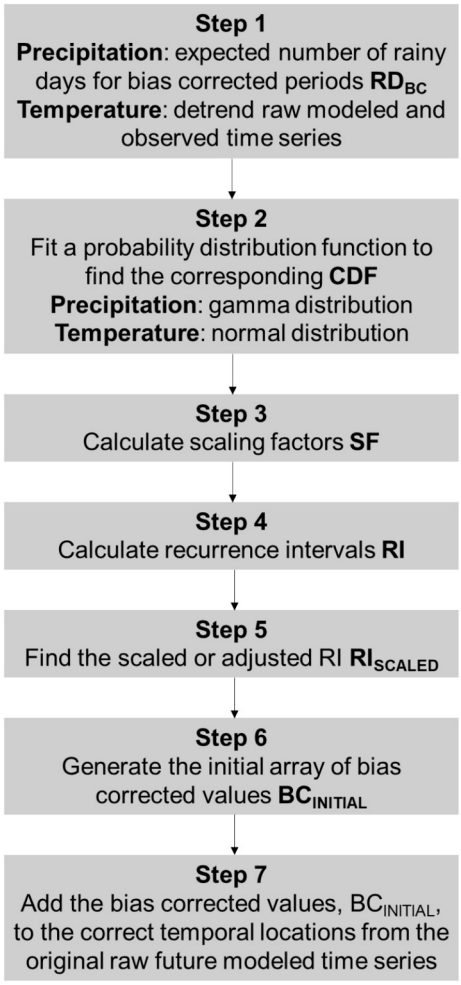

Fig. 3. Illustration of the seven key steps for SDM to do bias corrections for precipitation and temperature.

The period from 1981 to 2005 was set as the historical period and observation data (precipitation and temperature) in this period were collect from MSWEP and ERA5. Bias correction of the RCMs, was done for four periods, 1981–2005, 2025–2049, 2050–2074, and 2075–2099 as historical (Hist), near-future (NF), mid-future (MF) and far-future (FF) periods. Consequently the performance of bias corrected RCMs was done by running the hydrological model in the historical period.

3.2. Hydrological modeling

3.2.1. Model description

We use the HBV model as our hydrological model, one of the most flexible, computational efficient models that has been implemented in diverse range of climatic and physiographic regions (Beck et al., 2016; Zhang and Lindström, 2007). It has also been widely applied in various Ethiopian basins, including the three transboundary basins (Adera and Alfredsen, 2020; Ali et al., 2023; Jillo et al., 2017). The model is implemented on a daily time scale with inputs of climate variables i.e., precipitation and potential evapotranspiration. We derived the basin averaged precipitation from MSWEP (Table 2). Potential evapotranspiration was determined using the temperature-dependent Hargreaves equation. Since snow processes are absent in the three basins, the model incorporated routines for soil moisture, runoff response, and channel routing, regulated by nine model parameters outlined in Abraham et al. (2022). Further details on these parameters and their influence can be found in Abraham et al. (2022) and Beck et al. (2016). The model comprised both upper reservoir (soil moisture reservoir) and lower reservoir (groundwater reservoir) responsible for the temporal distribution of generated runoff. The lower reservoir acted as a simple linear reservoir, accumulating water through percolation from the upper reservoir and generating baseflow (Q_2), regulated by recession parameters. Additionally, the lower reservoir represents deeper groundwater storage, contributing to baseflow and sustaining the dry period flow. Conversely, the upper reservoir (soil moisture reservoir) controlled the drainage of both the quick flow component (Q_0) and the slow flow component (Q_1). The overall basin outflow (Q_T) was calculated by summing the volume of water discharged from the upper and lower reservoirs: $Q_T = Q_0 + Q_1 + Q_2$, and then is routed to the basin outlet.

3.2.2. Model calibration, validation and projection

Model calibration and validation were conducted within the Monte-Carlo scheme using daily observed streamflow data across the three basins. Using the Latin Hypercubic sampling, we generated 20,000 Monte-Carlo parameter sets. Kling–Gupta efficiency (KGE) (Gupta et al., 2009) and relative volume error (eR) were used as the performance measures (Eq. (1) and (2). Three distinct calibration criteria were employed to select the parameter ensemble that can well reproduce streamflow suitable for hydropower simulation in the three basins. These criteria include: i) parameter sets scoring KGE $\geq$ 0.8 for the total streamflow (Q_{Tot}), ii) parameter sets with a relatively small volume error for the total flow (eR Q_{Tot}) $\leq$ 5%, and iii) parameter sets with a relatively small volume error of high flow (eR Q_{75}) $\leq$ 5%. In this context, total flow (Q_{Tot}) encompasses the entire time series of streamflow, including both low and high flows, while high flow (Q_{75}) denotes flows exceeding the 75th percentile from the total flow. Calibration was done for 2006–2012, 1986–1991, and 1994–2002 for UBN, Omo, and Tekeze basins respectively and a warm up period of one year was considered to avoid the effect of initial conditions. Validation was carried out during another time period from 2013 to 2016, 1992–1994, and 2003–2007 for the UBN, Omo, and Tekeze basins, respectively. Ultimately, we chose parameter sets that adhere to the three-calibration rule and combine them to create a set of "combined parameters". Thus, each set of parameters in the "combined parameters" satisfy model performance in all

the three calibration criteria. These combined parameter sets may yield varying numbers of parameter sets across the three basins, providing a measure of parameter uncertainty. Employing these combined parameters and RCM climate forcings, we simulated streamflow and their associated uncertainties for historical (1981–2005) and three future periods (2025–2049, 2050–2074, and 2075–2099), respectively

$$\mathrm{KGE} = 1 - \sqrt{(r-1)^2 + (\alpha-1)^2 + (\beta-1)^2} \quad (1)$$

$$eR = \left|\frac{\overline{Qs,all} - \overline{Qo,all}}{\overline{Qo,all}}\right| * 100\% \quad (2)$$

where r, α, and β represent the linear correlation coefficient, the ratio of standard deviation and the ratio of mean between the simulation and observation, respectively. $\overline{Qs,all}$ and $\overline{Qo,all}$ are the mean values of the simulated and observed flow values, respectively.

3.3. Hydropower potential

Hydropower capacity is determined by the water release and hydraulic head. In this study we calculate hydropower capacity at the monthly scale using Eq. (3) and (4):

$$P = Q \times H \times \rho_w \times g \times \eta \quad (3)$$

$$E = P \times t \quad (4)$$

where P [MW] is the hydropower capacity, which is also constrained by the installed turbine capacity. Q [Mm^3/s] is the monthly mean water release through turbines. H [m] is the hydraulic head drop. ρ_w is the density of water, here it is set to 1000 kg/m^3. g is the gravity constant, which is set to 9.81 m/s^2. η [-] denotes the efficiency of turbines, which is 0.95 for the studied dams. E [MWh] is the energy, here hydropower electricity, produced by turbine generators. t [h] is the total hours of turbine operations.

Hydropower potential is the maximum hydropower energy that can be produced within a period of time through optimizing the policy for water release through turbines. To achieve that, we used the Reservoir package in R (Turner and Galelli, 2016; Wu et al., 2018), specifically we used the "dp_hydro" function. It has been used in other studies to quantify hydropower production, in particular, Cáceres et al. (2022) applied it to investigate potential hydropower and its contribution to mitigate climate risk in Africa. The "dp_hydro" function requires the time-series of inflow and reservoir evaporation rate as input and parameters regarding dam and reservoir properties (described in Table 1). Then it uses the built-in optimization method to determine the optimal time-series of water release (Q in Eq. (3) and the corresponding hydraulic head (H in Eq.3) in order to maximize the hydropower energy during a specific time period (hydropower potential).

The dynamic programming approach optimizes the water release from the reservoir to minimize the sum of the penalty costs incurred in long-term operation of the reservoir considering the storage constraints, mass balance and minimum water release, which then results in the optimal hydropower potential (Turner and Galelli, 2016).

$$S_{t+1} = S_t + Q_t - E_t - R_t - Q_{spill,t}, \text{ where } 0 \le S \le S_{cap}, R_{min,t} \le R_t \le S_t \quad (5)$$

$$C_t = [1 - \left(\frac{R_t}{D}\right)]^{\tau} \quad (6)$$

where S_t, Q_t, E_t, R_t, are $Q_{spill,t}$ represent the volume of water storage in the reservoir, inflow volume, evaporation loss volume, release volume and volume of water through spillway during the time step t in Mm^3, respectively. S_{cap} [Mm^3] and $R_{min,t}$ [Mm^3] denote the storage capacity of the reservoir and the minimum water release volume during time step t, respectively. C_t[-] is the penalty cost at time step t. D [Mm^3] is the target release. τ [-] is the penalty cost exponent, 2 is often used in academic studies.

The optimization returns the optimal sequence of releases for the input inflow time series by solving the following equation using the backwards recursive procedure (Turner and Galelli, 2016; Loucks et al., 2005).

$$f_t(S_t) = min\{C_t(S_t, Q_t, E_t, R_t, R_{min,t}) + f_{t+1}(S_{t+1})\} \forall S_t and t \in \{1, \cdots, t_n\} \quad (7)$$

where t_n is the last time step. The water release decision R_t is selected to minimize the current period cost C_t plus the future cost $f_{t+1}(S_{t+1})$.

Here, the built-in functions use dam and reservoir properties described in Table 1 to form the storage-hydraulic head-surface area relationship, and then this relationship is used to compute the dynamic storage and the corresponding hydraulic head and reservoir surface area. At the monthly temporal resolution, the following equations describe the built-in relationships between storage, hydraulic head and surface area:

$$c = \frac{2S_{cap}}{d_{max}A_{max}} \quad (8)$$

$$A(S) = \frac{2S_{cap}}{cd_{max}}\left(\frac{S_t}{S_{cap}}\right)^{1-c/2} \quad (9)$$

$$y(S) = d_{max}\left(\frac{S_t}{S_{cap}}\right)^{c/2} \quad (10)$$

$$H(S) = y(S) + y_{const} \quad (11)$$

$$y_{const} = H_{max} - d_{max} \quad (12)$$

where $H(S)$ [m], $y(S)$ [m] and $A(S)$ [km^2] represent the hydraulic head, water level and the surface area at storage S, respectively. d_{max} [m], H_{max} [m], and A_{max} [km^2] denote the maximum water depth, maximum hydraulic head, and the maximum surface area at the full storage of the reservoir, respectively. c [-] and y_{const} [m] are the constants for the specific reservoir.

Finally, the "dp_hydro" function outputs the optimized time-series of hydropower capacity, turbine water release, reservoir evaporation volume and spillway release. These form the main variables for our analysis, i.e., hydropower energy (Eq. (4) based on hydropower capacity, total water release (sum of the turbine water release and spillway release) and the reservoir evaporation volume.

To guarantee a certain amount of water available for the downstream of the dam, in this paper we introduce the monthly minimum water release. It is the minimum flow rate that should be released by the turbine for a specific month. Therefore, the actual water release to the downstream is then in the range of the monthly minimum water release and the maximum turbine release capacity and the available active storage in the reservoir (detailed calculation refers to Sect. 3.4). We achieve this by introducing water release constraints (Fig. 2) into the original Reservoir package to constrain the monthly minimum water release through the water release policy within the hydropower optimization for different scenarios in the next section. Inflow from the basin into the reservoir is simulated by the calibrated hydrological model using the corresponding area for the reservoir at the daily resolution, and afterwards aggregated into the monthly inflow.

3.4. Transboundary river management scenarios

To explore the cooperation possibilities between upstream (water use for hydropower) and downstream countries (e.g., water demand for irrigation), we introduce 11 water release scenarios for the hydropower dam operation covering the range from mostly beneficial for the upstream country to mostly beneficial for the downstream country. The key point is to achieve a balance between preserving natural river flow

regimes and minimizing adverse impacts on hydropower generation. It can be described by the following two steps:

Step 1: obtain the monthly pattern of natural flow into the reservoir. We calculated the long-term mean monthly flow for the three basins using 25-year historical streamflow. Then the contribution fraction of each month to the annual streamflow is calculated by Eq. (13):

$$f_{m,i} = \frac{\overline{Q}_{m,i}}{\sum_{i=1}^{12} \overline{Q}_{m,i}} \quad (13)$$

where $f_{m,i}$ [-] is fraction of the i-th month contribution to the annual total streamflow, $\overline{Q}_{m,i}$ [Mm^3/s] is the long-term mean of i-th month in the historical period, i is $1-12$ representing January to December.

Step 2: calculate the monthly water release for each scenario based on the previously derived monthly flow patterns. We generate these 11 scenarios through varying water release constraints. Scenario 1 is no constrains for water release, which is the best for the upstream country. It means that each month can release water in the range of 0 to the maximum release (considering the maximum turbine release capacity and the available active capacity of the reservoir). Scenario 2 is the 10% constraints for water release. Each month has to release at least 10% of the natural flow (10% $\times$ $f_{m,i}$ $\times$ long-term historical annual mean streamflow) of the corresponding month calculated in step 1. This means the real monthly water release is in the range of 10% of historical natural flow to the maximum release. Following this rule, Scenario 3 to Scenario 10 has the water release constraints from 20% to 90%. Scenario 11 has full constraints for water release, which is the best for the downstream country. It means that the water release follows the monthly pattern of the natural flow calculated in step 1, but taking account of the maximum release. Please also refer to the water release constraints illustration described in the scenarios and optimization of hydropower potential modeling in Fig. 2.

Taking the worst climate change scenario RCP8.5, with our 11 water release scenarios we aim to find a cooperation range that provide optimal hydropower and water release among the varying water release policies within this scenario spectrum to achieve a good balance between upstream hydropower production and downstream water use demand. Here, the good balance can be achieved, by selecting those scenarios among the scenario spectrums satisfying the maximum hydropower production for upstream and maximum water release to the downstream.

4. Results

4.1. Hydrological model performance

Fig. 4 shows the model parameter confinement procedure for the three studied basins. The combined simulation satisfying the three calibration rules (Sect. 3.2.2) was derived, retaining 87, 288, and 70 parameter sets from the initial 20,000 Monte-Carlo samples for UBN, Omo, and Tekeze, respectively (Fig. 4). It effectively narrows down the parameter uncertainty. The daily calibration demonstrates good performance with median KGE values of 0.85, 0.83, and 0.81 for UBN, Omo, and Tekeze, respectively (Table S3). Utilizing the optimized calibration parameters, model validation was conducted, resulting in good performance as well with daily median KGE values of 0.82, 0.76, and 0.85 for the three basins (Table S3). Furthermore, using the combined parameters, we evaluated the performances of five selected RCMs in historical periods (1981–2005). Despite lower KGE values of RCA_CSIRO for UBN and RCA_NorESM for Tekeze, the rest performs satisfactory on the monthly scale (Fig. S2).

Fig. 5 visualizes the daily streamflow simulations. The dynamics of observed low flow and high flow are well captured by the mean of the combined simulations in both calibration and validation periods. Meanwhile, the uncertainty is strongly reduced after calibration compared to all 20,000 Monte-Carlo simulations. It suggests that the combined parameter sets are adequate to be used to simulate historical and future streamflow for hydropower potential computations.

4.2. Future hydropower potential

Fig. 6 and Fig. S3 depict the relationship between energy production and water release from the dam to downstream under different scenarios. The energy production and water release values are the mean values from the five RCMs, while the uncertainty envelop of RCMs on annual energy is shown in Fig. S4. In general, when increasing the constraint of monthly water release, firstly we see a little decrease in energy production and a small increase in the actual water release to downstream. For instance, in the historical period, changing water release from no constraints to 40% constraints scenario of the historical monthly flow, the energy production declines by 3.0%, 2.3%, and 2.0% in GERD, Omo-Gibe III, and Tekeze respectively (Table S6). The fast decrease in energy production can be observed for all three sites beyond the 0% to 40% constraints range, while the total water release to downstream increases. In the historical period, when changing the water release pattern from most beneficial to the upstream country to most beneficial to the downstream country, the energy production is reduced by 4854.6, 1489.2, 136.1 GWh/year for the GERD, Omo-Gibe III, and

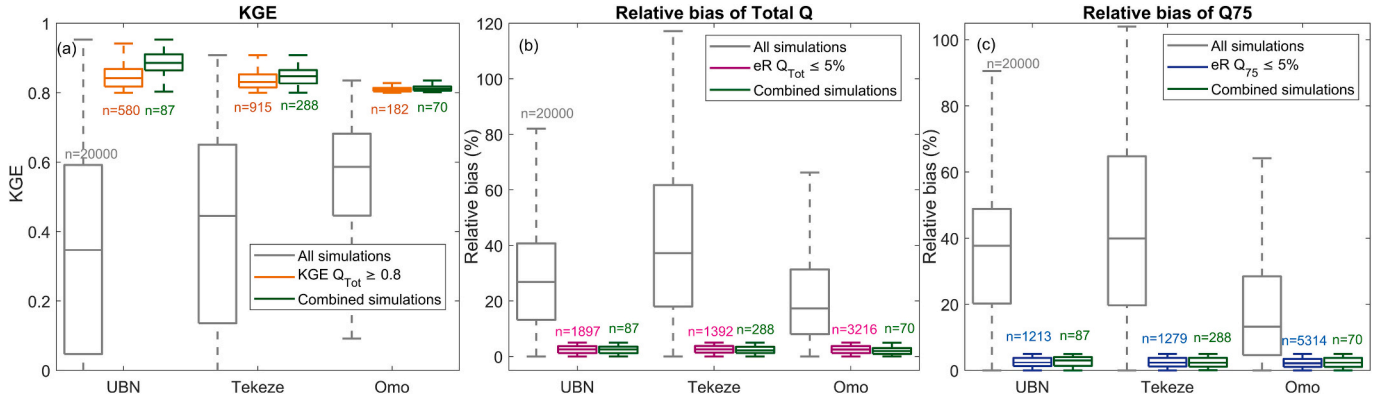

Fig. 4. Performance evaluation under three different calibration rules, a) general performance of the total flow for all and reduced simulations based on KGE (orange), b) relative volume error of total flow (Q_{Tot}) for all and reduced simulations based on eR (magenta) and c) relative volume error of high flows (Q_{75}) for all and reduced simulations based on eR (blue). The green color are parameters satisfying the three calibration criteria (Combined simulations). (For interpretation of the references to colour in this figure legend, the reader is referred to the web version of this article.)

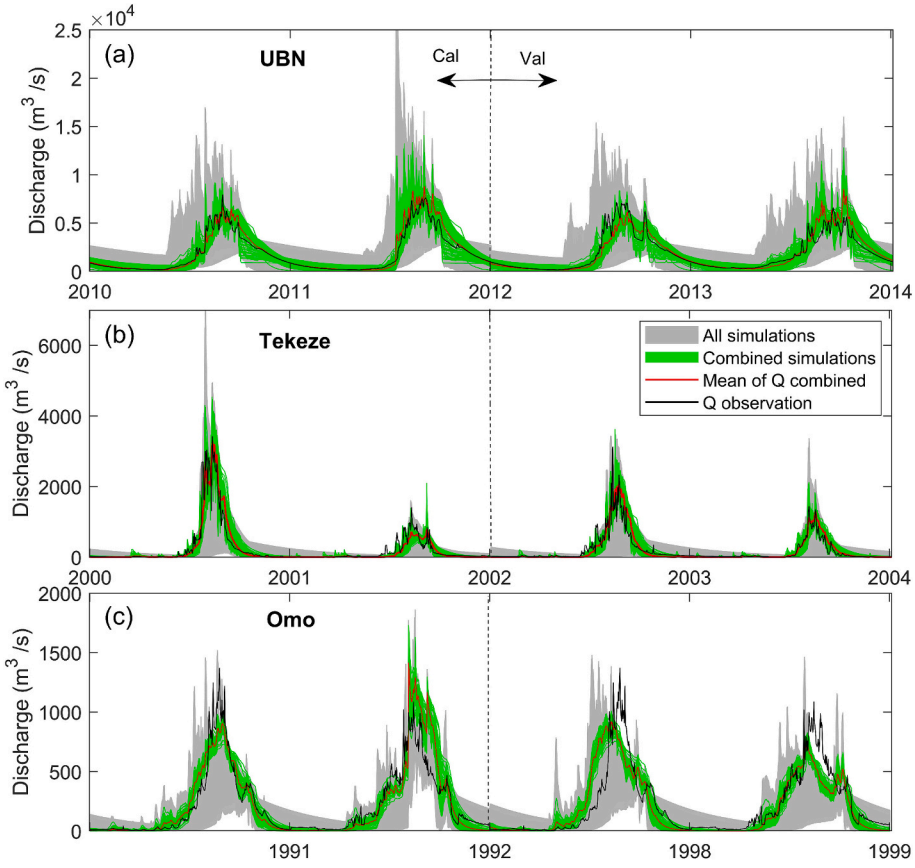

Fig. 5. Calibration and validation showing the entire 20,000 simulations (grey), and combined simulations from the three parameter selection rules (green) for the three transboundary rivers. For better visualization, we only show each two-year simulation for calibration and validation, respectively. (For interpretation of the references to colour in this figure legend, the reader is referred to the web version of this article.)

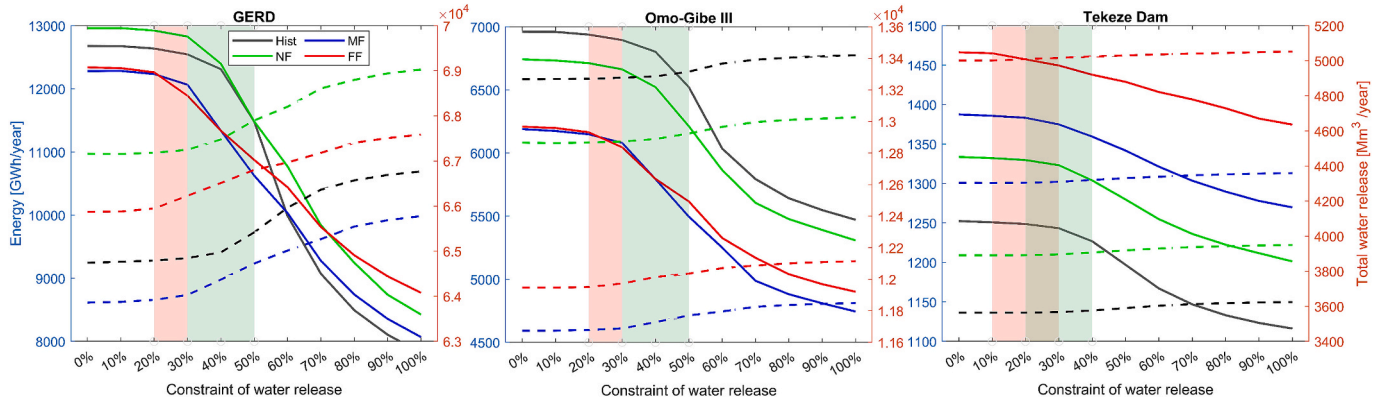

Fig. 6. Change of long-term mean annual energy production (solid line) and annual total water releases, the sum of release through spillway and turbines (dash line), in the historical (Hist) and three future (NF, MF, FF) periods under different scenarios of increasing constraints (from no constraints to full constraints) for water release, and the cooperation ranges of the historical (light green) and future (light red) periods. (For interpretation of the references to colour in this figure legend, the reader is referred to the web version of this article.)

Tekeze dams respectively. They correspond to a decrease of 38.0%, 21.4%, 10.9% for the three hydropower dams, respectively (Table S6).

The impact of climate change on the energy production and water release varies with each dam (Fig. 6). Energy production in GERD is projected to increase in the near-future (NF) by 2.2% compared to the historical periods and reduce for mid-future (MF) and far-future (FF) periods by 3.1% and 2.7% respectively under the no constraints water release scenario (Scenario 1). Hence, apart from the near-future period, simulations projected that GERD and Omo-Gibe III will have a decreased energy production and water release for the same scenario compared to the historical period, while Omo-Gibe III is predicted to have a distinct decline in the mid-future and far-future. Tekeze is predicted to have an increased energy production and water release due to the increase in the projected streamflow (Table S5). In Tekeze, under no constraints of water release (most beneficial to upstream) energy production have increased from the historical to the far-future periods by 17.1%. Under full constraints of water release (most beneficial to the downstream country, Scenario 11) energy production in Tekeze has increased by

23.2% from the historical to the far-future periods (Table S5). This is attributed to the projected increment in streamflow that would potentially maximize downstream release and energy production in the upstream. On the other hand, if keeping the same water release constraints as in the historical period in GERD and Omo-Gibe III, energy production will be reduced to certain extent in the future. For example, if maintaining water release to be 50% constraints of the historical monthly flow compared to no constraints (0%) to maximize energy production, the historical period reduces 1198.0 GWh/year, while the mid-future period reduces 1655.6 GWh/year for the GERD (Table S7).

Climate change has also resulted in the change of cooperation range from the historical to the future periods as shown by the shaded regions of light green and red colors (Fig. 6). For GERD and Omo-Gibe III the historical cooperation range is expected to be formed by maintaining the monthly water release in the range of 30%-50% of the historical monthly flow to the available reservoir storage (the light green shaded area in Fig. 6). For Tekeze, the historical cooperation range is expected from 20% to 40% of the historical monthly flow to the available reservoir storage. Climate change resulted in the shift of these cooperation ranges in the future periods. For instance, for the GERD and Omo-Gibe III the cooperation range shifted to the range of 20–30% of historical monthly flow as the minimum monthly water release threshold to satisfy the future periods energy production in Ethiopia (Fig. 6). However, for Tekeze the projected climate change has not significantly impacted the cooperation range. Therefore, with the impact of climate change, the upstream and downstream countries should adapt the cooperative strategy for hydropower production and water release according to the change of streamflow.

The monthly energy production pattern and its potential alterations in future periods under three representative water release scenarios are depicted in Fig. 7 and Fig. S5. Generally, the impact of the water release pattern on energy production is similar for historical and three future periods. They all show increasing energy production in the dry season (January to April) and decrease in the wet season (July to October) (Fig. S5). Notably, September emerges as the peak month for energy generation for the three dams. In the historical period, when increasing water release constraints from no constraints (S1) to 40% (S5), the energy production shows a decrease of 28.3% and 17.5% in GERD and Omo-Gibe III respectively for the peak month of September (Fig. 7). However, changing constraints for water release from 0% to 100% in the historical period for September results in a decline in energy production by 54.3%, 42.8%, and 20.2% in GERD, Omo-Gibe III, and Tekeze dam respectively (Fig. 7).

To better illustrate the climate change impact on energy production in the future periods, we have rearranged Fig. 7 and plotted in Fig. S5. This showed variable impact of climate change on energy production across the three dams, as illustrated in Fig. S5. When imposing the constraint of water release from 0% (S1) to 40% (S5), there is a decrease in energy production during the wet season from historical to the three future periods for GERD and Omo-Gibe III dams. For the three representative scenarios, Omo-Gibe III experiences a decline in energy production during the three future periods compared to the historical level in most months. This could be directly linked to the projected reduction in streamflow for future periods, as indicated in Table S4. Conversely, Tekeze dam exhibits an increasing mean monthly energy production during the three future periods compared to the historical level in all months. This increase is directly attributed to the rise in annual streamflow for future periods, as shown in Table S4.

4.3. Change in inflow to downstream countries

The monthly patterns of total water flowing from the turbine and spillway to the downstream, and its potential alterations in future periods under various water release scenarios, are presented in Fig. 8 and Fig. S6. The monthly mean values are the long-term averages for 25 years of historical data and three future periods (NF, MF, and FF). The water releases to the downstream were computed from the mass balance equation and hydropower calculations in Sect. 3.3. The result reveals that, when changing the water release from no constraints (Scenario 1) to full constraints (Scenario 11), future period water release to the downstream increases in the dry season and decreases in the wet season for the GERD (Fig. S6). During the historical period, increasing water release constraints from no constraint (0%) to medium constraint (40%) raised the mean monthly water release in the driest month (February) from 2011.9 Mm^3/month, 351.5 Mm^3/month, and 233.2 Mm^3/month to 4298.4 Mm^3/month, 863.1 Mm^3/month, and 266.4 Mm^3/month for GERD, Omo-Gibe III, and Tekeze, respectively—corresponding to 2.13, 2.45, and 1.14 times the original values (Fig. 8). Additionally, throughout the future periods, the same increasing pattern of water release was observed for the driest month (February), while increasing

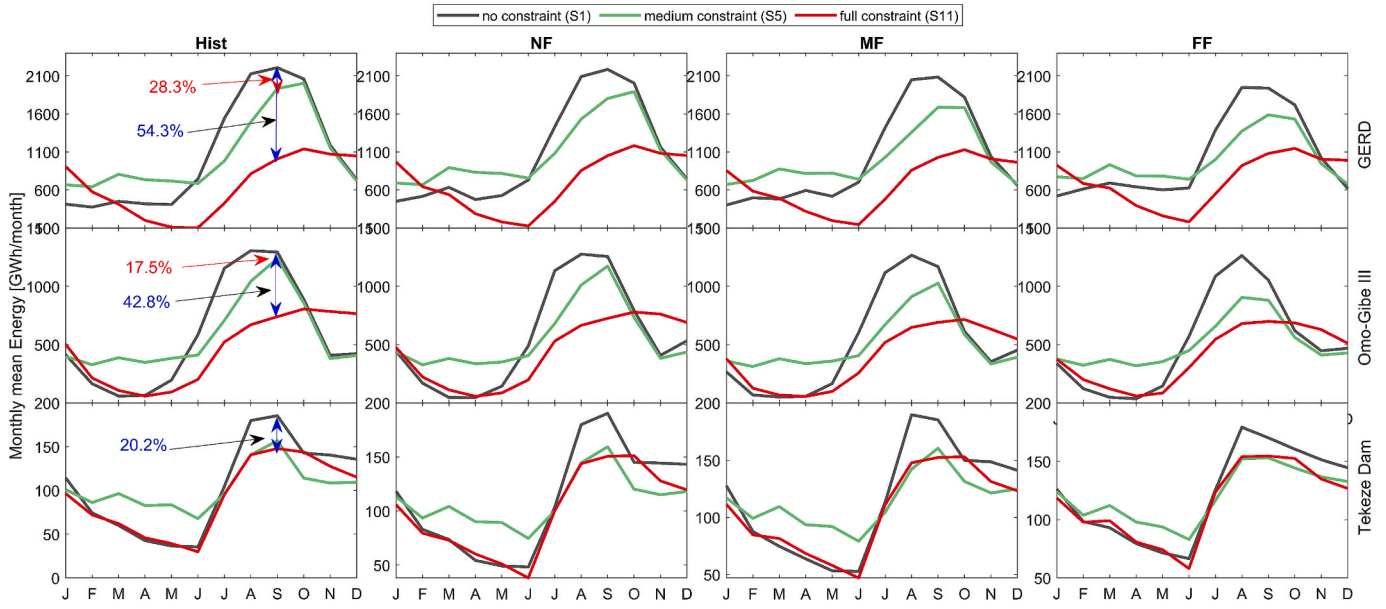

Fig. 7. Change of monthly mean energy under no constraints (Scenario 1), medium constraints (Scenario 5), and full constraints for water release (Scenario 11) in the historical (Hist) and three future periods (NF, MF, FF).

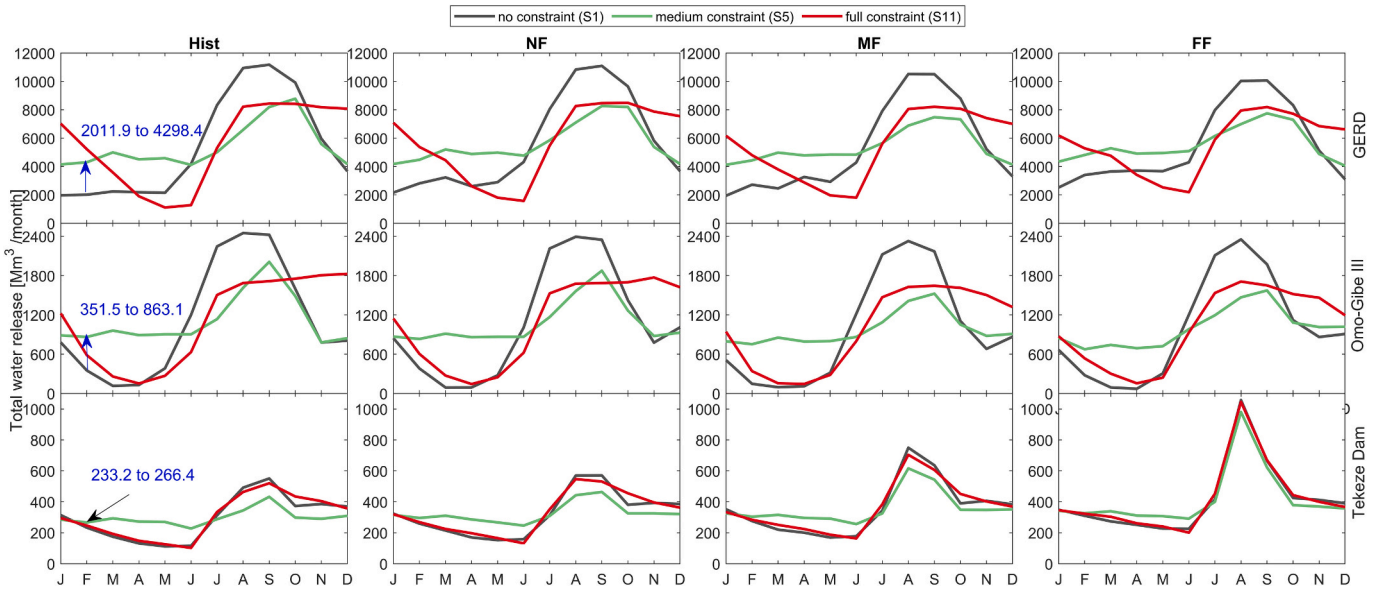

Fig. 8. Change of monthly mean total water release from the turbines and spillways to the downstream in the historical and three future periods under no constraints (Scenario 1), medium constraints (Scenario 5), and full constraints for water release (Scenario 11).

the constraints. On the other hand, water release in the wet season (July to October) showed reduction when increasing constraints from no constraints to medium and full constraints in all three dams.

The impact of climate change on the total water release during different seasons varies across the three dams (Fig. S6). For the no and medium constraints of water release scenarios, there is a decrease in total water release during the wet season from the historical period to the three future periods (NF, MF, and FF) in GERD and Omo-Gibe III. In contrast, Tekeze dam exhibits an increasing total water release during the three future periods compared to the historical level in all months for all water release scenarios.

4.4. Change in reservoir evaporation

Water release regulations affect the evaporation loss from reservoir (Fig. 9 and Fig. S7). In Ethiopia, the local dry season (January to April) is known for its high temperatures and evaporation rates. During this season, the monthly mean evaporation loss shows a moderate decrease in GERD and Omo-Gibe III for the historical periods when the water release is changed from 0% to 40% constraints (Fig. S7). However, a significant reduction in monthly mean evaporation loss during the historical period is observed in all three dams when switching to the full constraints scenario. For better illustration the scenario wise comparison of monthly evaporation patterns is shown in Fig. 9. Shifting from the scenario of no constraints (S1) of water release to full constraints (S11) in the historical periods, the monthly mean evaporation loss reduces for the peak month of March by 61.8%, 61.1% and 28.6% for GERD, Omo-Gibe III and Tekeze dams, respectively.

Under climate change increase in evaporation loss from the reservoir is projected for most water release scenarios, due to the projected increase of temperature (Fig. S7). The difference is that the increased loss from the historical to the future period is slightly larger for the scenario

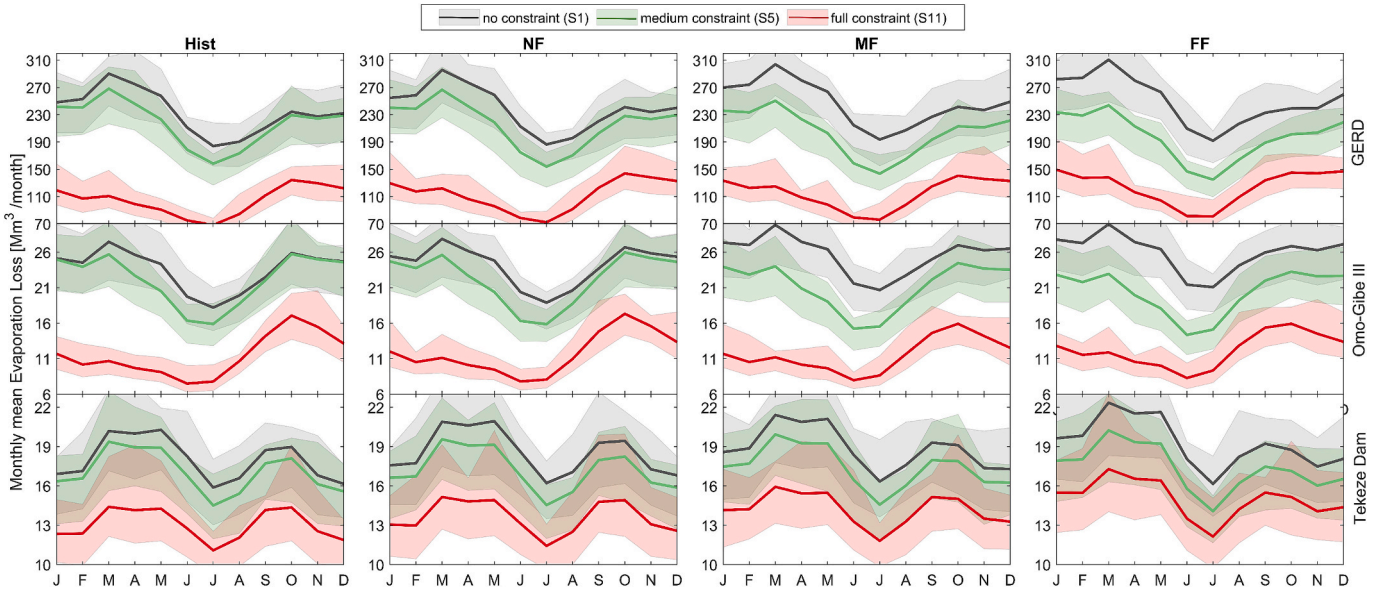

Fig. 9. Change of monthly mean evaporation loss from the reservoir and their uncertainty interval in the historical and future periods under no constraints (Scenario 1), medium constraints for water release (Scenario 5) and full constraints for water release (Scenario 11).

with no constraints for water release compared to reduced and full constraints scenarios. For example, under no constraints, evaporation loss changes from 290.3 Mm^3/month, 27.5 Mm^3/month and 20.2 Mm^3/month to 310.6 Mm^3/month, 29.9 Mm^3/month and 22.3 Mm^3/month in March from historical to the far-future period for GERD, Omo-Gibe III, Tekeze, respectively. This means through changing water release patterns, there might be a possibility of saving water from evaporation.

5. Discussion

5.1. Implications of the results

The future period's streamflow projections have important implications for hydropower production and cooperation, particularly in the context of transboundary basins. Due to high hydroclimatic variabilities in the three studied basins, the projected streamflow shows correspondingly different patterns of variability. In UBN, the near-future and far-future periods showed increments in streamflow from their historical values, despite a reduction in the mid-future (Table S4). The Omo River showed a consistent reduction of future-period streamflow (Table S4). Conversely, the Tekeze River has shown a consistent increment in streamflow for the three future periods from its historical values. The future period's streamflow projections, which are based on a comprehensive selection of RCM, are in agreement with other previous studies in the three study sites (Adera and Alfredsen, 2020; Bombelli et al., 2021; Paulos et al., 2022; Teferi et al., 2015). Despite the agreements on reservoir operation rules, changes in future-period streamflow volume can affect the cooperation levels required between the upstream and downstream countries. Thus, the future variabilities of inflow volume suggest the adaptability of reservoir operation rules also for future conditions. Even though difficulties exist in accurately projecting future-period extreme events (floods and droughts), their added effect on dam operations, particularly from transboundary rivers, is undeniable. Despite these challenges, a scenario-wise simulation of reservoir operations, considering the future period's streamflow variabilities, can enable an understanding of the level of cooperation required in the future. Under different water release scenarios, it is possible to figure out where both upstream and downstream countries can cooperate in the historical period and how it may be impacted by climate change.

The hydropower projection from the GERD, Omo-Gibe III, and Tekeze dams has followed a similar pattern to the streamflow. The future period's annual energy from GERD is projected to increase in the near-future by 2.2% and to reduce by 3.1% and 2.7% during the mid-future and far-future periods, respectively, under the no-constraints water release scenario (Fig. 6). With increasing water release constraints to 40% (Scenario 5), the energy production in GERD increases by 0.7% in the near-future and declines by 7.9% and 9.9% in the mid-future and far-future periods, respectively. Following the reducing patterns of future period streamflow, the annual and monthly energy production in Omo-Gibe III showed a projected decline across all water release constraints (Fig. S5). A regional study has also further confirmed a projected reduction of the future available water for hydropower production in Omo-Gibe III (Paulos et al., 2022). For Tekeze, due to a consistent increase in streamflow, the future energy is projected to consistently increase even under increasing constraints until full constraints (Scenario 11) (Fig. 6). This implies that even under increasing constraints for water release (0% to 100%), the reservoir remains stable enough to generate the required energy each month. Furthermore, the future period's increasing streamflow is able to sustain energy production. For Tekeze, a similar study has also projected an increase of hydropower potential up to 30% under climate scenarios, suggesting resilient energy production in future periods (Abera et al., 2018).

This study showed that the water release pattern can largely influence the total hydropower potential and actual downstream water flow in dry and wet seasons. Therefore, cooperation is needed between upstream and downstream countries for their energy and water demand. This study introduced a novel approach that enables one to find a cooperation range among the different scenarios of water release. Furthermore, this approach can also enable one to find suitable cooperation zones for future periods under climate change. This study has particular implications for both upstream and downstream countries by providing a cooperation range to choose. Generally, this cooperation range is expected to balance energy production and water releases. For instance, for GERD and Omo-Gibe III, maintaining the minimum water release threshold within 30%-50% of the monthly natural flow constitutes the cooperation range in the historical period (Fig. 6). For Tekeze, the expected cooperation range in the historical period is within 20%-40%. However, with the influence of climate change, this cooperation range should be adapted. For instance, for GERD and Omo-Gibe III in the future, this cooperation range shifts to 20–30% of the historical monthly flow as the minimum monthly water release threshold to satisfy energy production in Ethiopia (Fig. 6). However, for Tekeze, this cooperation range in the future is not too much affected by climate change. Increasing the minimum monthly water release threshold, as described in the cooperation range, the energy production in the historical period only has a very small decline. This implies that adapted cooperation is required for GERD and Omo-Gibe III; however, Tekeze remains stable under future climate change. Increasing water release constraints from 0% to 40%, the actual water release in the driest month (February) increases by 2.13, 2.45, and 1.14 times for GERD, Omo-Gibe III, and Tekeze, which will increase water release to the downstream, particularly important in dry seasons.

5.2. Uncertainties and future directions

Managing transboundary river flow alongside the development of hydropower projects poses challenges due to differences in development and conservation priorities. Downstream and upstream water demand, as well as changes in transboundary river flow, are usually the causes of conflict. However, downstream flow reduction may not solely be attributed to upstream hydropower development projects; climate change and variability also significantly contribute to this issue (Hoang et al., 2019; Piman et al., 2013; Yun et al., 2020). On the other hand, the future growth in population and economy, along with future hydropower development plans, can complicate the operation and management of shared water bodies. While this study provided an approach for cooperative water release options, it is not without uncertainties and limitations that should be addressed in upcoming studies. The primary sources of uncertainty are within the hydroclimatic projections and the model structure. The regional modeling can be subject to uncertainties from future emissions, climate sensitivity, and hydrological responses in the region. Furthermore, the modeling framework in this study has not included population growth scenarios, economic development, or the future energy demand, all of which will affect water allocation. In addition, this study has not included water uses, such as abstraction for water supply, which could affect the water available for energy generation and downstream release. Incorporation of these factors, together with climate change and future reservoir operation, can provide a comprehensive assessment of the impact. The cooperation ranges we provide are also significantly affected by future climate alteration. Adapting these cooperation ranges under climate change is essential for both upstream and downstream countries in managing transboundary rivers. Nevertheless, further methodological refinements are necessary, incorporating critical factors such as projected population growth, economic development trajectories, and evolving hydropower expansion strategies. Such enhancements would strengthen integrated hydropower management frameworks and foster cooperative transboundary river governance.

6. Conclusions

This study performed a projection of hydropower potential and

water releases of future periods for three dams in the transboundary rivers: the GERD, Omo-Gibe III, and Tekeze dams in Ethiopia. Streamflow was projected using the calibrated HBV hydrological model based on a careful climate model selection as well as a robust bias correction. After introducing a factor to control the water release constraints into the R package 'Reservoir', hydropower potential was calculated under different water release scenarios. They range from those most beneficial to the upstream country (Ethiopia) to those most beneficial to the downstream countries. Within this range of 11 scenarios, we focused on finding the cooperative range that can optimize energy production in Ethiopia and water release to downstream countries. This cooperation range is expected to balance energy production and water releases.

Our study indicates that by increasing water release constraints, the hydropower potential declines slowly in the early phase. However, there is a significant increase in water release to downstream during the dry season. This suggests that altering the water release pattern can maintain hydropower production while boosting actual water release during the dry season. It implies that a well-balanced cooperation range can accommodate both upstream and downstream demands. The findings propose that for the GERD and Omo-Gibe III, maintaining the minimum water release threshold within 30%-50% of the monthly natural flow constitutes the cooperation range in the historical period. However, for Tekeze, the expected cooperation range is within 20%-40%. Nevertheless, climate change will affect this cooperation range in the future. For example, for the GERD and Omo-Gibe III, this cooperation range is expected to reduce to 20%-30% in future periods. However, increased streamflow projections for future periods in Tekeze suggest that climate change will slightly impact this cooperation range. Regarding the GERD, maintaining the minimum water release threshold at 50% of the historical monthly natural flow, compared to operating without any constraints to maximize energy production, reduces energy production by 1198.0 GWh/year in the historical period and by 1655.6 GWh/year in the mid-future period. This indicates that both upstream and downstream countries should adapt their cooperative strategy in response to the impact of climate change.

Energy production in the three dams responds differently during wet and dry seasons under changing climate. In the case of the GERD, energy production surpasses historical levels during the dry season in future periods from no constraints to medium constraints for water release. Omo-Gibe III experiences a decline in energy production during the three future periods compared to historical levels in most months. However, the Tekeze dam exhibits an increasing mean monthly energy production during the three future periods compared to historical levels in all months.

To enhance cooperation in transboundary projects, it is essential to consider climate change, as it affects the required cooperation levels in future periods. Our assessment indicates that the cooperation ranges we provided are influenced by future climate change. Therefore, water release constraints in adapting to these cooperation ranges under climate change is crucial for energy development and water requirements in transboundary basins.

CRediT authorship contribution statement

Tesfalem Abraham: Writing – review & editing, Writing – original draft, Visualization, Validation, Methodology, Formal analysis, Data curation, Conceptualization. **Tunde Olarinoye:** Writing – review & editing, Visualization. **Andreas Hartmann:** Writing – review & editing, Visualization, Supervision. **Harrie-Jan Hendricks Franssen:** Writing – review & editing, Visualization, Supervision. **Yan Liu:** Writing – review & editing, Writing – original draft, Visualization, Validation, Methodology, Formal analysis, Conceptualization.

Declaration of competing interest

The authors declare that they have no known competing financial interests or personal relationships that could have appeared to influence the work reported in this paper.

Acknowledgements

We are grateful to Ethiopia's Ministry of Water, Irrigation, and Electricity for providing the essential streamflow data used in our research. Additionally, we would like to acknowledge the Earth System Grid Federation (ESGF) at the Deutsches Klimarechenzentrum (DKRZ) for providing the regional climate model data for Africa. Open Access funding was organized by Projekt DEAL.

Appendix A. Supplementary data

Supplementary data to this article can be found online at https://doi.org/10.1016/j.jhydrol.2026.135111.

Data availability

The data utilized in the analysis of the study's findings can be obtained upon reasonable request from the corresponding author. Precipitation is from the MSWEP v2 product, which was described by Beck et al. (2019) and can be accessed by filling the request form via https://www.gloh2o.org/mswep/. Historical temperature data is from ERA5, which was described by Cucchi et al. (2022) and can be downloaded by specifying the variable "Near-surface air temperature" and time periods via https://cds.climate.copernicus.eu/cdsapp#!/dataset/10.24381/cds.20d54e34?tab=form. Streamflow data can be obtained from Ali et al. (2023) through their provided link. All regional climate data from the CORDEX-AFRICA group can be downloaded from https://esgf-metagrid.cloud.dkrz.de/search/cordex-dkrz/, where one need to specify in the "General": Project = "CORDEX", Domain = "AFR-44", in the "Identifiers": Experiment = "historical" or "rcp85", in the "Classifications": Ensemble = "r1i1p1", Time Frequency = "day", Variable = "pr" or "tas", or "tasmax", or "tasmin".

References

Abera, F.F., Asfaw, D.H., Engida, A.N., Melesse, A.M., 2018. Optimal operation of hydropower reservoirs under climate change: the case of Tekeze reservoir. Eastern Nile. Water (switzerland) 10, 273. https://doi.org/10.3390/w10030273.

Abraham, T., Gelete, G., Liu, Y., 2025. Assessing the flood and drought regulation capacity of dams in a changing climate: an application to the largest hydropower dam in africa. Earth Syst. Environ. 9. https://doi.org/10.1007/s41748-025-00815-8.

Abraham, T., Liu, Y., 2025. Climate change impact on effective water use for hydropower generation of the Grand Ethiopian Renaissance Dam. Theor. Appl. Climatol. 156, 312. https://doi.org/10.1007/s00704-025-05538-4.

Abraham, T., Liu, Y., Tekleab, S., Hartmann, A., 2022. Prediction at ungauged catchments through parameter optimization and uncertainty estimation to quantify the regional water balance of the ethiopian rift valley lake basin. Hydrology 9, 1–27. https://doi.org/10.3390/hydrology9080150.

Adera, A.G., Alfredsen, K.T., 2020. Climate change and hydrological analysis of tekeze river basin ethiopia: implication for potential hydropower production. J. Water Clim. Chang. 11, 744–759. https://doi.org/10.2166/wcc.2019.203.

Ali, A.M., Melsen, L.A., Teuling, A.J., 2023. Inferring reservoir filling strategies under limited-data-availability conditions using hydrological modeling and Earth observations: the case of the Grand Ethiopian Renaissance Dam (GERD). Hydrol. Earth Syst. Sci. 27, 4057–4086. https://doi.org/10.5194/hess-27-4057-2023.

Anebo, A., Woldesenbet, T.A., Ayele, G., 2023. Estimating reservoir evaporation using numerical weather prediction: a case study of the gibe iii reservoir in Ethiopia. Environ. Res. Commun. 5, 085010. https://doi.org/10.1088/2515-7620/acf02d.

Aniley, E., Gashaw, T., Abraham, T., Fetene, S., Bayabil, H.K., Worqlul, A.W., Van, P.R., Dile, Y.T., Chukalla, A.D., Haileslassie, A., 2023. Evaluating the performances of gridded satellite / reanalysis products in representing the rainfall climatology of Ethiopia. Geocarto Int. 38, 2278329. https://doi.org/10.1080/10106049.2023.2278329.

Annys, S., Ghebreyohannes, T., Nyssen, J., 2020. Impact of hydropower dam operation and management on downstream hydrogeomorphology in semi-arid environments (Tekeze, Northern Ethiopia). Water (Switzerland) 12, 2237. https://doi.org/10.3390/w12082237.

Antonio, P., Cagiano, A., Eugenio, Z., Giuseppe, P., Claudio, R., 2018. Design and Operation of Gibe III Power Waterways, in: Hydro 2018 - Progress through Partnership. Gdansk, Poland.

Basheer, M., Nechifor, V., Calzadilla, A., Gebrechorkos, S., Pritchard, D., Forsythe, N., Gonzalez, J.M., Sheffield, J., Fowler, H.J., Harou, J.J., 2023. Cooperative adaptive management of the Nile River with climate and socio-economic uncertainties. Nat. Clim. Chang. 13, 48–57. https://doi.org/10.1038/s41558-022-01556-6.

Basheer, M., Nechifor, V., Calzadilla, A., Siddig, K., Etichia, M., Whittington, D., Hulme, D., Harou, J.J., 2021. Collaborative management of the Grand Ethiopian Renaissance Dam increases economic benefits and resilience. Nat. Commun. 12, 1–12. https://doi.org/10.1038/s41467-021-25877-w.

Beck, H.E., van Dijk, A.I.J.M., de Roo, A., Miralles, D.G., McVicar, T.R., Schellekens, J., Bruijnzeel, L.A., 2016. Global-scale regionalization of hydrologic model parameters. Water Resour. Res. 52, 3599–3622. https://doi.org/10.1002/2015WR018247.

Beck, H.E., Wood, E.F., Pan, M., Fisher, C.K., Miralles, D.G., Van Dijk, A.I.J.M., McVicar, T.R., Adler, R.F., 2019. MSWep v2 Global 3-hourly 0.1° precipitation: methodology and quantitative assessment. Bull. Am. Meteorol. Soc. 100, 473–500. https://doi.org/10.1175/BAMS-D-17-0138.1.

Bombelli, G.M., Tomiet, S., Bianchi, A., Bocchiola, D., 2021. Impact of prospective climate change scenarios upon hydropower potential of Ethiopia in GERD and GIBE Dams. Water 13, 716. https://doi.org/10.3390/w13050716.

Cáceres, A.L., Jaramillo, P., Matthews, H.S., Samaras, C., Nijssen, B., 2022. Potential hydropower contribution to mitigate climate risk and build resilience in Africa. Nat. Clim. Chang. 12, 719–727. https://doi.org/10.1038/s41558-022-01413-6.

Carrillo, J., Hernández-Barrera, S., Expósito, F.J., Díaz, J.P., González, A., Pérez, J.C., 2023. The uneven impact of climate change on drought with elevation in the Canary Islands. NPJ Clim. Atmos. Sci. 6, 31. https://doi.org/10.1038/s41612-023-00358-7.

Casanueva, A., Herrera, S., Iturbide, M., Lange, S., Jury, M., Dosio, A., Maraun, D., Gutiérrez, J.M., 2020. Testing bias adjustment methods for regional climate change applications under observational uncertainty and resolution mismatch. Atmos. Sci. Lett. 21, e978.

Chen, J., Guo, Y., Li, M., 2021. Constructivism on Transboundary Cooperation of Rhine River Basin, in: 5th International Seminar on Education, Management and Social Sciences (ISEMSS 2021). Doi: 10.2991/assehr.k.210806.032.

Dallison, R.J.H., Patil, S.D., Williams, A.P., 2021. Impacts of climate change on future water availability for hydropower and public water supply in Wales, UK. J. Hydrol.: Reg. Stud. 36, 100866. https://doi.org/10.1016/j.ejrh.2021.100866.

El-Magd, I.H.A., Ali, E.M., 2012. Estimation of the evaporative losses from Lake Nasser, Egypt using optical satellite imagery. Int. J. Digit. Earth 5, 133–146. https://doi.org/10.1080/17538947.2011.586442.

Gerlak, A.K., Saguier, M., Mills-Novoa, M., Fearnside, P.M., Albrecht, T.R., 2020. Dams, chinese investments, and EIAs: a race to the bottom in South America? Ambio 49, 156–164. https://doi.org/10.1007/s13280-018-01145-y.

Ghoreishi, M., Elshorbagy, A., Razavi, S., Blöschl, G., Sivapalan, M., 2023. Cooperation in a transboundary river basin: a large-scale socio-hydrological model of the Eastern Nile. Hydrol. Earth Syst. Sci. 27, 1201–1219. https://doi.org/10.5194/hess-27-1201-2023.

Giordano, M., Drieschova, A., Duncan, J.A., Sayama, Y., De Stefano, L., Wolf, A.T., 2014. A review of the evolution and state of transboundary freshwater treaties. Int. Environ. Agreements Polit. Law Econ. 14, 245–264. https://doi.org/10.1007/s10784-013-9211-8.

Gou, J., Miao, C., Duan, Q., Zhang, Q., Guo, X., Su, T., 2022. Seasonality and impact factor analysis of streamflow sensitivity to climate change across China. Earth's Futur. 10, e2022EF003062. https://doi.org/10.1029/2022EF003062.

Gupta, H.V., Kling, H., Yilmaz, K.K., Martinez, G.F., 2009. Decomposition of the mean squared error and NSE performance criteria: implications for improving hydrological modelling. J. Hydrol. 377, 80–91. https://doi.org/10.1016/j.jhydrol.2009.08.003.

Hargreaves, G., Samni, Z., 1982. Estimation of potential evapotranspiration. J. Irrig. Drain. Div. 108, 223–230.

Hennig, T., 2016. Damming the transnational Ayeyarwady basin. hydropower and the water-energy nexus. Renew. Sustain. Energy Rev. 65, 1232–1246. https://doi.org/10.1016/j.rser.2016.07.048.

Hoang, L.P., van Vliet, M.T.H., Kummu, M., Lauri, H., Koponen, J., Supit, I., Leemans, R., Kabat, P., Ludwig, F., 2019. The Mekong's future flows under multiple drivers: how climate change, hydropower developments and irrigation expansions drive hydrological changes. Sci. Total Environ. 649, 601–609. https://doi.org/10.1016/j.scitotenv.2018.08.160.

ICOLD, 2023. World Register of Dams. General Synthesis. [April 2023]; Available from: https://www.icold-cigb.org/article/GB/world_register/general_synthesis /general-synthesis. [WWW Document]. https://www.icold-cigb.org/article/GB/world_register/general_synthesis/general-synthesis.

IEA, 2019. IRENA, UNSD WB. WHO. Tracking sdg 7. The Energy Progress Report; 2019.

IPCC, 2022. Climate Change 2022: Impacts, Adaptation and Vulnerability. Contribution of Working Group II to the Sixth Assessment Report of the Intergovernmental Panel on Climate Change. Cambridge University Press, Cambridge, UK and New York, NY, USA. https://doi.org/doi:10.1017/9781009325844.

Jillo, A.Y., Demissie, S.S., Viglione, A., Asfaw, D.H., Sivapalan, M., Demissie, S.S., Viglione, A., Asfaw, D.H., Sivapalan, M., 2017. Characterization of regional variability of seasonal water balance within Omo-Ghibe River Basin. Ethiopia. Hydrol. Sci. J. 62, 1200–1215. https://doi.org/10.1080/02626667.2017.1313419.

Korjonen-Kuusipuro, K., 2011. Critical water: negotiating the Vuoksi River in 1940. Water Hist. 3, 169–186. https://doi.org/10.1007/s12685-011-0035-6.

Lazin, R., Shen, X., Moges, S., Anagnostou, E., 2023. The role of Renaissance dam in reducing hydrological extremes in the Upper Blue Nile Basin: current and future climate scenarios. J. Hydrol. 616, 128753. https://doi.org/10.1016/j.jhydrol.2022.128753.

Llamosas, C., Sovacool, B.K., 2021. The future of hydropower? a systematic review of the drivers, benefits and governance dynamics of transboundary dams. Renew. Sustain. Energy Rev. 137, 110495. https://doi.org/10.1016/j.rser.2020.110495.

Ly, K., Metternicht, G., Marshall, L., 2022. Transboundary river basins: Scenarios of hydropower development and operation under extreme climate conditions. Sci. Total Environ. 803, 149828. https://doi.org/10.1016/j.scitotenv.2021.149828.

Munia, H.A., Guillaume, J.H.A., Wada, Y., Veldkamp, T., Virkki, V., Kummu, M., 2020. Future transboundary water stress and its drivers under climate change: a global study. Earth's Futur. 8, 1–21. https://doi.org/10.1029/2019EF001321.

NBI, 2012. State of the River Nile Basin 2012. Entebbe: Nile Basin Initiative.

Paulos, T., Kranjac-berisavijevic, G., Abagale, F.K., 2022. Impact of climate change on future availability of water for irrigation and hydropower generation in the Omo-Gibe Basin of Ethiopia. J. Hydrol.: Reg. Stud. 44, 101254. https://doi.org/10.1016/j.ejrh.2022.101254.

Peila, D., Viggiani, G., &, Celestino, T. (Eds.)., 2019. Tunnels and Underground Cities. Engineering and Innovation Meet Archaeology, Architecture and Art: Proceedings of the WTC 2019 ITA-AITES World Tunnel Congress (WTC 2019), May 3-9, 2019, Naples, Italy (1st ed.). CRC Press. https://doi.org/https://doi.org/10.1201/9780429424441.

Piman, T., Lennaerts, T., Southalack, P., 2013. Assessment of hydrological changes in the lower Mekong Basin from Basin-Wide development scenarios. Hydrol. Process. 27, 2115–2125. https://doi.org/10.1002/hyp.9764.

Qin, P., Xu, H., Liu, M., Du, L., Xiao, C., Liu, L., Tarroja, B., 2020. Climate change impacts on three Gorges Reservoir impoundment and hydropower generation. J. Hydrol. 580, 123922. https://doi.org/10.1016/j.jhydrol.2019.123922.

Ribeiro, W.C., 2017. Shared use of transboundary water resources in la Plata River Basin: Utopia or reality? Ambient. E Soc. 20, 257–270. https://doi.org/10.1590/1809-4422ASOCEx0005V2032017.

Shu, J., Qu, J., Motha, R., Xu, J.C., Dong, D.F., 2018. Impacts of climate change on hydropower development and sustainability: a review Impacts of climate change on hydropower development and sustainability: a review. Earth Environ. Sci. Pap. 163, 012126. https://doi.org/10.1088/1755-1315/163/1/012126.

Sinha, R., 2006. Two neighbours and a treaty: baglihar project in hot waters. Econ. Polit. Wkly. 41, 606–608. https://doi.org/10.2307/4417834.

Soukhaphon, A., Baird, I.G., Hogan, Z.S., 2021. The impacts of hydropower dams in the mekong river basin: a review. Water (switzerland) 13, 1–18. https://doi.org/10.3390/w13030265.

Switanek, M.B., Troch, P.A., Castro, C.L., Leuprecht, A., Chang, H.-I., Mukherjee, R., Demaria, E.M.C., 2017. Scaled distribution mapping: a bias correction method that preserves raw climate model projected changes. Hydrol. Earth Syst. Sci. 21, 2649–2666. https://doi.org/10.5194/hess-21-2649-2017.

Teferi, M., Willems, P., Block, P., 2015. Implications of climate change on hydrological extremes in the Blue Nile basin: a review. J. Hydrol.: Reg. Stud. 4, 280–293. https://doi.org/10.1016/j.ejrh.2015.07.001.

Turner, S.W.D., Galelli, S., 2016. Water supply sensitivity to climate change: an R package for implementing reservoir storage analysis in global and regional impact studies. Environ Model Softw. 76, 13–19. https://doi.org/10.1016/j.envsoft.2015.11.007.

Wei, Y., Wei, J., Li, G., Wu, S., Yu, D., Ghoreishi, M., Lu, Y., 2022. A socio-hydrological framework for understanding conflict and cooperation with respect to transboundary rivers. Hydrol. Earth Syst. Sci. 26, 2131–2146. https://doi.org/10.5194/hess-26-2131-2022.

Wheeler, K.G., Hall, J.W., Zagona, E., Whittington, D., 2020. Understanding and managing new risks on the Nile with the Grand Ethiopian Renaissance Dam. Nat. Commun. 11, 5222. https://doi.org/10.1038/s41467-020-19089-x.

Wu, X., Cheng, C., Lund, J.R., Niu, W., Miao, S., 2018. Stochastic dynamic programming for hydropower reservoir operations with multiple local optima. J. Hydrol. 564, 712–722. https://doi.org/10.1016/j.jhydrol.2018.07.026.

Yuan, L., He, W., Degefu, D.M., Liao, Z., Wu, X., An, M., Zhang, Z., Ramsey, T.S., 2020. Transboundary water sharing problem; a theoretical analysis using evolutionary game and system dynamics. J. Hydrol. 582, 124521. https://doi.org/10.1016/j.jhydrol.2019.124521.

Yun, X., Tang, Q., Wang, J., Liu, X., Zhang, Y., Lu, H., Wang, Y., Zhang, L., Chen, D., 2020. Impacts of climate change and reservoir operation on streamflow and flood characteristics in the Lancang-Mekong River Basin. J. Hydrol. 590, 125472. https://doi.org/10.1016/j.jhydrol.2020.125472.

Zarfl, C., Lumsdon, A.E., Berlekamp, J., Tydecks, L., Tockner, K., 2015. A global boom in hydropower dam construction. Aquat. Sci. 77, 161–170. https://doi.org/10.1007/s00027-014-0377-0.

Zhang, X., Lindström, G., 2007. A comparative study of a swedish and a chinese hydrological model. JAWRA J. Am. Water Resour. Assoc. 32, 985–994. https://doi.org/10.1111/j.1752-1688.1996.tb04067.x.

Zhao, G., Merder, J., Ballard, T.C., Michalak, A.M., 2023. Warming may offset impact of precipitation changes on riverine nitrogen loading. PNAS 120, e2220616120. https://doi.org/10.1073/pnas.2220616120.

Zhong, W., Guo, J., Chen, L., Zhou, J., Zhang, J., Wang, D., 2020. Future hydropower generation prediction of large-scale reservoirs in the upper Yangtze River basin under climate change. J. Hydrol. 588, 125013. https://doi.org/10.1016/j.jhydrol.2020.125013.